and anions, which allows the water molecule to escape easily from the crystal lattice in the more voluminous $[Ir(H_2O)(NH_3)_5]^{3+}$ complexes.

Since there are few studies of solid-state reactions of Rh(III) and Ir(III), we hope, in the future, to study this apparent anomaly in other complexes of $[Rh(H_2O)(NH_3)_5]^{3+}$ and $[Ir(H_2O)(NH_3)_5]^{3+}$ with several other entering anions to compare with the behavior of the known Co(III) analogues. It is hoped that such work will determine whether the relative size of the ions and the free space is effectively more important than the *Dq* contribution of the metal ion.

**Acknowledgment.** We are very grateful for the Financial Support of "Fondo Nacional para el Desarrollo de la Investigación Cientifica, CAYCIT, No. 360(81)".

**Registry No.** I, 75058-08-1; II, 95267-24-6; III, 60897-44-1; IV, 95267-25-7; V, 95267-26-8; VI, 95267-27-9; VII, 95267-28-0; VIII, 95267-29-1; IX, 95247-02-2; X, 95247-03-3; XI, 95247-04-4; XII, 95247-05-5; XIII, 95247-06-6.

**Supplementary Material Available:** Tables of computational parameters for $[M(H_2O)(NH_3)_5][Cr(CN)_6]$ (M = Rh, Ir) from both nonisothermal and isothermal measurements (2 pages). Ordering information is given on any current masthead page.

Contribution from the Laboratoire de Chimie de Coordination, Université de Provence, the Service de Cristallochimie, and the Laboratoire d'Électronique, Centre St. Jérôme, 13397 Marseille Cedex 13, France

# Structure and Conductivity of Chloro(phthalocyaninato)zinc Single Crystals

MIREILLE MOSSOYAN-DENEUX,*† DAVID BENLIAN,† MARCEL PIERROT,‡ ANDRÉ FOURNEL,§ and JEAN PIERRE SORBIER§

*Received June 6, 1984*

A new crystalline form of oxidized zinc phthalocyanine has been prepared by electrolysis in organic solvent. X-ray analysis of single crystals of ZnPcCl, grown at a Pt anode, shows helical stacks of bimolecular aggregates that allow, in different ways, inter-aromatic-ring overlaps. We can notice both an exceptionally large outward axial shift of the zinc and a rigorous planarity of the Pc ring. FT-IR spectra of both ZnPc and ZnPcCl confirm the structural differences between the two materials. The integral oxidation number and the structure are consistent with the intrinsic semiconductor properties demonstrated by the resistivity measurements. The new material, ZnPcCl, is characterized by a rather narrow gap and a transition point at ~230 K.

Reports, including X-ray crystal structure studies, have been published on molecular conductors and molecular semiconductors. Some of these compounds are metal phthalocyanines modified by oxidative insertion of iodine.[1-4]

Among these, few attempts of crystal growth at an electrode are mentioned, in spite of the well-known electrochemistry of macrocyclic complexes. The present paper describes an original compound obtained by electrooxidation from an organic solution. This compound has remarkable electronic properties, comparable to those of halogen-doped phases. The X-ray structure of the material shows striking similarities to that of the metallic conductor NiPcI.[1] The vibrational spectra and the conductivity data of the new material are discussed in accordance with the structural features and in comparison with other results published on similar compounds.

## Experimental Section

**Preparation.** ZnPc, obtained by the usual synthesis,[5] was purified by repetitive sublimation and precipitation from a $H_2SO_4$ solution. Electrolysis was performed on a two-electrode system. Amperostatic regulation was maintained for about 200 h, to collect large enough crystals from the anode. Some pulverulent material with identical properties settled on the bottom of the vessel.

No elemental analysis could be done, but sweeping microscopic examination showed well-formed crystals on which X-ray analysis by energy gave invariably the ratio Zn/Cl = 1.

**Crystal Structure.** A 0.4 × 0.15 × 0.6 mm³ crystal with no particular feature was selected, and a precession chamber study (Mo K$\alpha$, $\lambda$ = 0.70 Å) gave the space group *P4/nnc* (No. 126[6]). Systematic extinctions are found for *hk*0 ($h + k = 2n + 1$), 0*kl* ($k + l = 2n + 1$), and *hhl* ($l = 2n + 1$). Parameters have been refined on an automatic diffractometer (Enraf-Nonius CAD4 with a graphite monochromator). The unit cell dimensions and volume are $a$ = 13.85 (1) Å, $c$ = 13.09 (1) Å, and $V$ = 2511 Å³. With the theoretical formula $ZnC_{32}H_{16}N_8Cl$ and for four molecules per unit cell, the calculated density of 1.62 agrees with the observed density of 1.58 obtained by flotation of the crystal in $ZnCl_2$ solutions. Data were collected with a $\omega$-2$\theta$ scan ($\theta_{max}$ = 27°). Intensity was controlled (maximum deviation <1%) on three standard reflections checked at 3600-s intervals. The orientation of the crystal was verified every 100 measurements. A total of 1200 data having $F_o^2 > 3\sigma(F_o^2)$ were used for initial refinements. A total of 1014 reflections *hkl*, *khl* were

**Table I.** Summary of Crystal Data and Intensity Collection

| | |
|---|---|
| compd | $ZnC_{32}H_{16}N_8Cl$ |
| cryst dimens, mm | 0.4 × 0.15 × 0.6 |
| space group | *P4/nnc* (No. 126) |
| $a$, Å | 13.85 (1) |
| $c$, Å | 13.09 (1) |
| $V$, Å³ | 2511 |
| $Z$ | 4 |
| density, g/cm³ | 1.62 (calcd)<br>1.58 (obsd) |
| radiation | graphite-monochromated Mo K$\alpha$ ($\lambda$ = 0.707 Å) |
| $\mu$, cm$^{-1}$ | 110 |
| scan | $\omega$-2$\theta$, $\theta_{max}$ = 27° |
| scan angle | 0.8 + 0.35 tan $\theta$ |
| slit aperture | 2.0 + 0.5 tan $\theta$ |
| $t_{max}$, s | 120 |
| unique data with $F_o^2 > 3\sigma F_o^2$ | 665 (after averaging Friedel pairs) |
| $R_I$ | 0.098 |
| $R_w$ | 0.11 |

**Table II.** Positional Parameters and Their Estimated Standard Deviations

| atom | $x$ | $y$ | $z$ |
|---|---|---|---|
| Zn(1) | 0.250 | 0.250 | 0.5840 (4) |
| Cl(1) | 0.250 | 0.250 | 0.4041 (6) |
| N(1) | 0.189 (1) | 0.123 (1) | 0.630 (2) |
| N(2) | 0.332 (1) | 0.020 (1) | 0.628 (2) |
| C(1) | 0.237 (1) | 0.036 (1) | 0.629 (2) |
| C(2) | 0.165 (1) | -0.043 (1) | 0.627 (2) |
| C(3) | 0.176 (1) | -0.142 (1) | 0.627 (2) |
| C(4) | 0.092 (2) | 0.197 (1) | 0.632 (3) |
| C(5) | 0.002 (2) | 0.155 (1) | 0.630 (2) |
| C(6) | -0.011 (1) | -0.055 (1) | 0.629 (2) |
| C(7) | 0.072 (1) | -0.000 (1) | 0.628 (2) |
| C(8) | 0.092 (1) | 0.104 (1) | 0.630 (1) |

† Laboratoire de Chimie de Coordination, Université de Provence.
‡ Service de Cristallochimie.
§ Laboratoire d'Electronique.

(1) Schramm, C. J.; Scaringe, R. P.; Stojakovic, D. R.; Hoffman, B. M.; Iber, J. A.; Marks, T. J. *J. Am. Chem. Soc.* **1980**, *102*, 6702.

0020-1669/85/1324-1878$01.50/0 

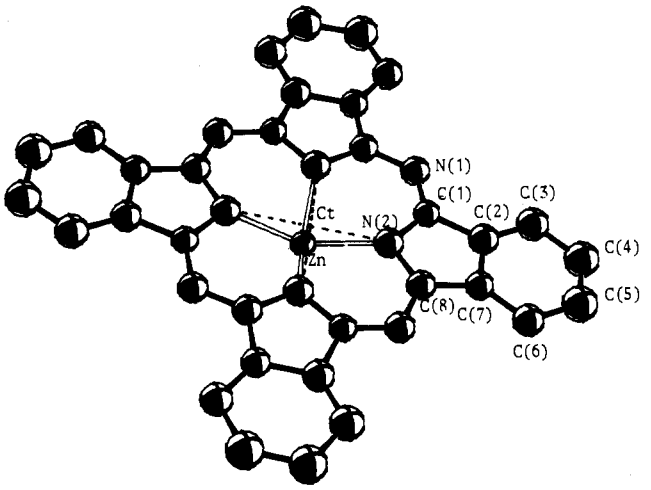


**Figure 1.** ORTEP diagram of the oxidized molecule showing the numbering scheme.

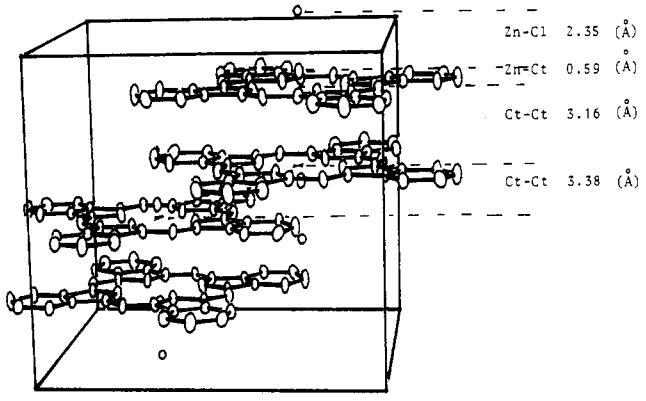


**Figure 2.** ORTEP drawing, view along the *a* axis, showing the interplanar distances in the stacking.

averaged. For symmetric reflections $R_I = 0.028$. Then, 665 independent unique reflections remained. The structure was solved by combining the Patterson function and the results from the MULTAN program[7] to give the coordinates for Zn and Cl with a reliability factor of $R = 0.30$. Other atoms were sited by Fourier synthesis. Full-matrix least-squares refinement gave $R = 0.10$ (with an anisotropic thermal agitation factor for each atom). The last refinements were carried after placing H atoms in their theoretical positions. Then agreement factors are

$$R = \sum(|F_o| - |F_c|)/\sum|F_o| = 0.098$$

$$R_w = [\sum w(|F_o| - |F_c|)^2/\sum w(|F_o|)^2]^{1/2} = 0.11$$

the function to minimize being $\sum w(|F_o| - |F_c|)^2$. Experimental data are given in Table I; positional parameters are listed in Table II.

**Infrared Measurements.** Infrared spectra have been recorded on a Nicolet 7099 FT spectrometer as KBr (1600–400 $cm^{-1}$) and polyethylene (400–80 $cm^{-1}$) pellets.

**Resistivity Measurements.** The resistivity measurement is performed by using the well-known four-probe method when the size of samples is larger than 1.5 mm; with smaller samples the measure is performed with two probes only. The contacts are obtained by cementing a gold wire ($\Phi \approx 15$ $\mu$m) with silver paste.

The activation energy is obtained as the slope of log $R$ vs. $1/T$. As multiple measurements have been performed, we can check that the same activation energy is given by four-probe or two-probe devices as well as by the direct-current or alternating-current (1 kHz) methods.

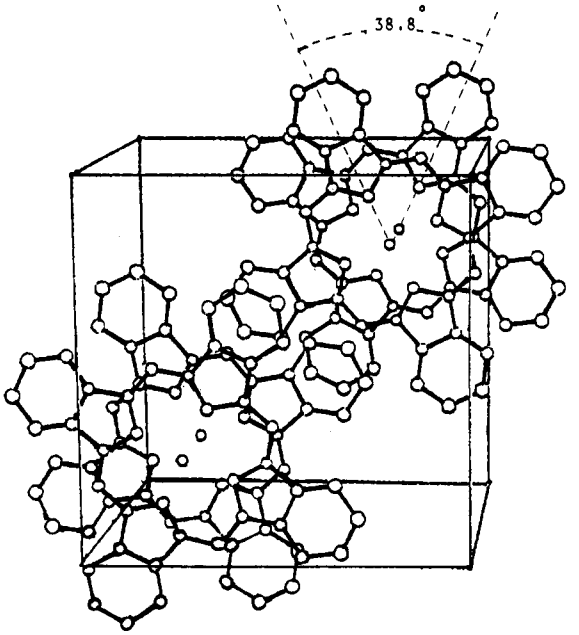


**Figure 3.** ORTEP drawing, view along the *c* axis, showing the staggered position of successive phthalocyanines.

**Table III.** Bond Distances (Å)[a]

| | | | |
|---|---|---|---|
| N(1)–C(1) | 1.380 (8) | C(3)–C(4) | 1.405 (11) |
| N(1)–C(8) | 1.381 (8) | C(4)–C(5) | 1.371 (12) |
| N(2)–C(1) | 1.332 (9) | C(5)–C(6) | 1.399 (11) |
| C(1)–C(2) | 1.479 (9) | C(6)–C(7) | 1.370 (8) |
| C(2)–C(3) | 1.370 (9) | C(7)–C(8) | 1.470 (9) |
| C(2)–C(7) | 1.422 (10) | | |

[a] Numbers in parentheses are estimated standard deviations in the least significant digits.

**Table IV.** Bond Angles (deg)[a]

| | | | |
|---|---|---|---|
| C(1)–N(1)–C(8) | 107.1 (6) | C(3)–C(4)–C(5) | 121.0 (7) |
| N(1)–C(1)–N(2) | 127.5 (6) | C(4)–C(5)–C(6) | 123.2 (7) |
| N(1)–C(1)–C(2) | 109.5 (6) | C(5)–C(6)–C(7) | 115.7 (8) |
| N(2)–C(1)–C(2) | 122.9 (6) | C(2)–C(7)–C(6) | 121.9 (7) |
| C(1)–C(2)–C(3) | 131.3 (7) | C(2)–C(7)–C(8) | 104.1 (6) |
| C(1)–C(2)–C(7) | 107.3 (6) | C(6)–C(7)–C(8) | 133.9 (7) |
| C(3)–C(2)–C(7) | 121.3 (7) | N(1)–C(8)–C(7) | 111.9 (6) |
| C(2)–C(3)–C(4) | 116.8 (8) | | |

[a] Numbers in parentheses are estimated standard deviations in the least significant digits.

## Results and Discussion

**Crystal Structure.** In Figures 1–3 the numbering of atoms and ORTEP views of the unit cell are shown. Alternate stacks of dimer units are organized in a helical geometry along the tetragonal axis. The Pc rings are set with respect to each other in a remarkable parallel staggered position, which is similar to the $NiPcI_{1.0}$ case:[1] staggering angle 38.8°, distances (Å) Ct–Ct′ = 3.16, $C_1$–$C_1$′ = 3.18, $C_8$–$C_8$′ = 3.16 (Ct = center of the square formed by the four pyrrolic nitrogens). Figures 2 and 3 show the essential features of the relative position of the cycles. Zn atoms lay 0.59 Å outside the ligand plane, at a distance of 2.35 Å from Cl axial ligands. Bond lengths and angles are given in Tables III and IV. The geometry of the $Zn_2Pc_2$ entity is compared those to other complexes with known structures in Table V.

In five-coordinate porphyrins or phthalocyanines reported in the literature,[8-12] the metal is located outside the equatorial plane

(2) Dirk, C. W.; Inabe, T.; Schoch, K. F., Jr.; Marks, T. J. *J. Am. Chem. Soc.* **1983**, *105*, 1539.
(3) Diel, B. N.; Inabe, T.; Lyding, J. W.; Schoch, K. F., Jr.; Kannewurf, C. R.; Marks, T. J. *J. Am. Chem. Soc.* **1983**, *105*, 1567.
(4) Kuznesof, P. M.; Wynne, K. J. *J. Chem. Soc., Chem. Commun.* **1980**, 121.
(5) Barret, P. A.; Dent, C. E.; Linstead, R. P. *J. Chem. Soc.* **1936**, 1719.
(6) "International Tables for X-ray Crystallography"; Kynoch Press: Birmingham, England, 1965.
(7) Main, P.; Woolfson, M. H.; Germain, G. "Multan, a System of Computer Programmes for the Automatic Solution of a Crystal Structure from X-ray Diffraction Data", Universities of York, England, and Louvain, Belgium, 1978.
(8) Kobayashi, T.; Ashida, T.; Uyeda, N.; Suito, E.; Kakudo, M. *Bull. Chem. Soc. Jpn.* **1971**, *44*, 2095.
(9) Spaulding, L. D.; Eller, P. G.; Bertrand, J. A.; Felton, R. H. *J. Am. Chem. Soc.* **1974**, *96*, 982.

**Table V.** Comparison of the Bond Distances (Å) in Similar Compounds

| | $NiPcI_{1.0}$[1] | ZnPc[25] | ZnPcCl | ZnPc(*n*-HxNH$_2$)[8] | Zn(TPP)$ClO_4$[9] | pyZnTpyP[10] | PyrZnOEP[11] | Zn(TPP)$H_2O$[12] | PbPc[14] |
|---|---|---|---|---|---|---|---|---|---|
| N(2)–C(1) | 1.379 (12) | 1.369 (3) | 1.380 (8) | 1.38 | 1.35 (1) | 1.369 (5) | 1.366 (1) | 1.38 | 1.375 |
| N(1)–C(1) | 1.320 (9) | 1.333 (3) | 1.332 (9) | 1.34 | 1.40 | 1.406 (5) | 1.390 (6) | | 1.36 |
| C(1)–C(2) | 1.458 (7) | 1.455 (3) | 1.474 (9) | 1.47 | 1.43 (1) | 1.447 (4) | 1.452 (6) | 1.42 | 1.49 |
| C(2)–C(3) | 1.387 (7) | 1.393 (3) | 1.370 (9) | 1.46 | | | | | 1.39 |
| C(3)–C(4) | 1.388 (6) | 1.390 (3) | 1.402 (11) | 1.42 | | | | | 1.44 |
| C(4)–C(5) | 1.394 (10) | 1.395 (4) | 1.371 (12) | 1.40 | | | | | 1.38 |
| C(2)–C(7) | 1.392 (10) | 1.400 (3) | 1.422 (10) | 1.43 | 1.39 (2) | 1.355 | 1.353 | 1.37 | 1.45 |
| Ct[a]–N(2) | 1.887 (6) | 1.980 | 1.946 | 2.005 | 2.046 (10) | 2.047 (12) | 2.043 (2) | 2.04 | 2.173 |
| M–N(2) | 1.887 (6) | 1.980 | 2.034 | 2.061 | 2.076 (8) | 2.073 | 2.067 (6) | 2.050 | 2.21 |
| M–Ct | 0 | 0 | 0.59 | 0.480 | 0.347 (9) | 0.33 | 0.31 | 0.19 (2) | 0.4 |
| | | | 2.35 | 2.178 | 2.079 | 2.143 | 2.200 | 2.20 | |
| dist between two planes | 3.15 | | 3.16 | 3.51 | 3.8 | | 3.41 | | |

[a] Ct is the center of the square formed by the four pyrrolic nitrogens.

**Table VI.** Least-Squares Planes

Deviations from Planes (Å)

| | plane 1 | esd | plane 2 | esd | plane 3 | esd |
|---|---|---|---|---|---|---|
| Zn | 0.586 | 0.006 | | | | |
| Cl | 2.94 | 0.008 | | | | |
| N1 | −0.011 | 0.020 | 0.006 | 0.020 | −0.073 | 0.020 |
| N2 | −0.002 | 0.020 | 0.002 | 0.020 | −0.060 | 0.020 |
| C1 | −0.011 | 0.022 | −0.009 | 0.022 | −0.061 | 0.022 |
| C2 | 0.026 | 0.021 | 0.008 | 0.021 | 0.000 | 0.021 |
| C3 | 0.025 | 0.032 | | | 0.017 | 0.032 |
| C4 | −0.034 | 0.042 | | | −0.021 | 0.042 |
| C5 | −0.008 | 0.031 | | | 0.007 | 0.031 |
| C6 | 0.014 | 0.027 | | | 0.011 | 0.027 |
| C7 | 0.009 | 0.021 | −0.005 | 0.021 | −0.014 | 0.021 |
| C8 | 0.009 | 0.019 | −0.000 | 0.019 | −0.055 | 0.019 |

Angles (deg) between Least-Squares Planes

| plane | plane | dihedral angle |
|---|---|---|
| 1 | 2 | 0.1 |
| 1 | 3 | 1.0 |
| 2 | 3 | 1.8 |

Equations of Planes[a]

plane 1 (macrocycle): $-0.0034x + 0.0006y - 1.000z + 8.2395 = 0$
plane 2 (pyrrolic cycle: $0.0006x + 0.0151y - 0.9999z + 8.2203 = 0$
plane 3 (benzenic cycle): $-0.0118x - 0.0139y - 0.9998z + 8.2227 = 0$

[a] $x$, $y$, and $z$ are orthogonalized coordinates.

formed by the four pyrrolic nitrogen atoms and, moreover, the cyclic ligand is significantly puckered in a tentlike geometry. Dihedral angles between adjacent pyrrole rings vary from 4.3 to 9.1° in Zn(TPP)$ClO_4$ and 7.4° in Zn(TPyrP)Pyr.[11]

In ZnPcCl no atom of the macrocycle deviates from the geometric plane by more than the estimated standard deviation (Table VI). Each benzopyrrole group is planar with a maximum deviation of 0.01 Å. Dihedral angles between the mean plane and the pyrrolic groups and in each benzopyrrole are very small.

As happens in all MPcL five-coordinate complexes in comparison with the four-coordinate MPc molecule, distances are altered in the Pc ring. All benzene C–C distances increase in the tentlike MPcL complexes. In ZnPcCl, their mean value remains very close to that in ZnPc ($\beta$ form)[13] (1.391–1.395), but it is worth noticing that they are alternatively longer and shorter. Such an alternation is observed in PbPc[13] (Table V). In comparison to those of similar five-coordinate compounds, one notes that bond distances in ZnPcCl are extreme: the four pyrrolic nitrogens are only 1.946 Å apart from the center Ct, and this is the smallest distance observed in any compound in the series. In this case, oxidation induces the maximum shrinking of the central core and extrusion of the metal along the axis. The Zn–Cl distance is in the average of weak polar bond lengths observed both in tetrahedral Zn complexes[14] and in M–Cl bonds of macrocyclic derivatives such as chlorohemin.[15] The distance between Cl and the nearest peripheral hydrogen in the unit cell is 2.86 Å. Therefore, one expects little interaction.

The stacking of $Zn_2Pc_2Cl_2$ blocks along the helix holds the plane-to-plane distance (3.38 Å) consistent with an electronic interaction. Aza bridges lay 3.40 Å apart from the C(5) carbon of the vicinal Pc ring (Figure 3).

**Table VII.** Conductivity Parameters for Some Phthalocyanines

| compd | $\sigma_{rt}$, $\Omega^{-1}$ cm$^{-1}$ | energy gap, eV | ref |
|---|---|---|---|
| NiPcI | 550[b] | | 1 |
| $(AlPcFI_x)_n$ I/F = 0.76 | 0.24[a] | 0.05 | 24 |
| I/F = 3.3 | 3.4[a] | 0.017 | 24 |
| $(GaPcFI_x)_n$ I/Ga = 0.97 | 0.072[a] | 0.03 | 24 |
| I/Ga = 2.1 | 0.15[a] | 0.04 | 24 |
| $[(GePcO)I_{1.94}]_n$ | $[(GePcO)I_{1.94}]_n$ | 0.05 | 25 |
| $[(SnPcO)I_{5.5}]_n$ | $2 \times 10^{-4}$ [a] | 0.68 | 25 |
| $[(SiPcO)I_{1.40}]_n$ | $2 \times 10^{-1}$ [a] | 0.04 | 25 |
| $[(SiPcO)I_{1.55}]_n$ | 1.4[a] | 0.028 | 3 |
| $[(SiPcO)Br_{1.12}]_n$ | $9.5 \times 10^{-1}$ [a] | 0.022 | 3 |
| ZnPc | $10^{-14}$ [b] | | 17 |
| ZnPcCl | $1 \times 10^{-1}$ [b] | 0.16 | this work |
| ZnPcCl | $1 \times 10^{-2}$ [a] | | this work |

[a] Conductivity measurements for pressed-powder pellets. [b] Conductivity measurements for monocrystals.

**Conductivity Measurements.** Among the published data, the measurements on $NiPcI_{1.0}$ were performed on single crystals. In all other cases compacted powder samples have been used. In general, insertion of iodine improves the conductivity in great proportions but the sample remains of semiconductive type. $NiPcI_{1.0}$ shows an unambiguous metallic conduction both in the single crystals and in compacted powder samples, well before any alteration of the solid could be suspected at higher temperatures. Our results are shown in Table VII compared to selected data from the literature.

ZnPcCl shows much higher conductivity ($10^{-1}$ $\Omega^{-1}$ cm$^{-1}$) than the starting material ($10^{-14}$ $\Omega^{-1}$ cm$^{-1}$).[17]

Most of our measurements have been done on single crystals of rather reduced size (~2 mm). Usually the conductivity in polycrystalline pellets is lower by about 2 orders of magnitude. A few checks on such samples have shown us a decrease in the range of $10^{-1}$.

In Figure 4 are grouped plots of the resistance $R$ vs. $10^3/T$ for our ZnPcCl samples. At high temperatures ($T > 230$ K), all plots

(10) Collins, D. M.; Hoard, J. L. *J. Am. Chem. Soc.* **1970**, *92*, 3761.
(11) Cullen, D. L.; Meyer, E. F., Jr. *Acta Crystallogr., Sect. B: Struct. Crystallogr. Cryst. Chem.* **1976**, *B32*, 2259.
(12) Glick, M. D.; Cohen, G. H.; Hoard, J. L. *J. Am. Chem. Soc.* **1967**, *89*, 1996.
(13) Scheidt, W. R.; Dow, W. *J. Am. Chem. Soc.* **1977**, *99*, 1101.
(14) Ukei, K. *Acta Crystallogr., Sect. B: Struct. Crystallogr. Cryst. Chem.* **1973**, *B29*, 2290.
(15) Wells, A. F. "Structural Inorganic Chemistry", 4th ed.; Clarendon Press: Oxford, England, 1975.
(16) Koenig, D. F. *Acta Crystallogr.* **1965**, *18*, 663.
(17) Aoyagi, Y.; Masuda, K.; Namba, S. *J. Phys. Soc. Jpn.* **1971**, *31* (1), 164.

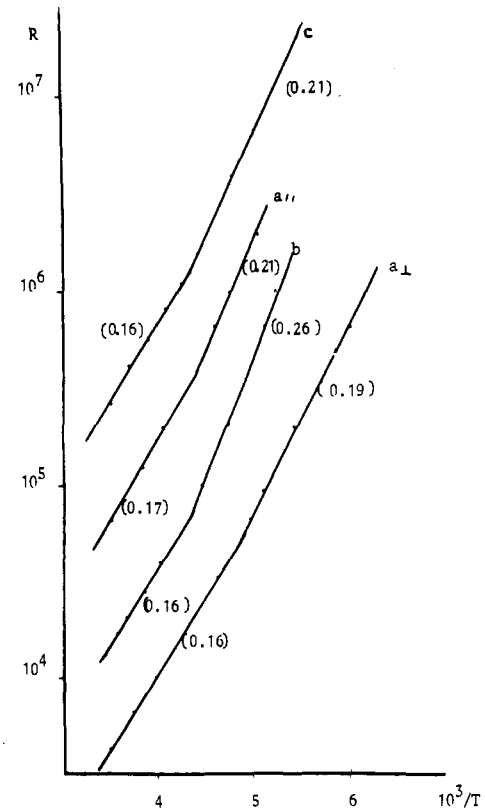


**Figure 4.** Plots of $R$ vs. $10^3/T$ for some crystals (a,b,c) from different batches. For crystal a, measures are made in both parallel and perpendicular directions to the stacking axis. The values in parentheses are the slopes of log $R$ vs. $1/T$, the activation energy (eV).

give the same gap, 0.16 ± 0.01 eV, with good linearity. At temperatures below 230 K, linearity is kept good but the experimental gaps vary in the 0.19–0.26-eV range. This may be due either to crystallization defects in the grown samples or to phase transitions in the solid. Attempts to characterize anisotropic behavior gave parallel plots in both directions and were not conclusive (Figure 4, $a_{\parallel}$ and $a_{\perp}$) due to the limited size of the samples. More experiments on much larger and well-formed samples would answer these questions and are currently under way.

All halogen-doped phthalocyanines showing a good conductivity have a nonintegral formal oxidation state and are stacked in a column of parallel phthalocyanine rings. Linear chains of iodine run parallel to the stack. Integrated or segregated stack crystals with an integral oxidation state are resistors or semiconductors with room-temperature conductivities below $10^{-3}$ $\Omega^{-1}$ cm$^{-1}$.[18] Whangbo et al.[19] have shown that, in halogen-doped metal phthalocyanine polymers, the electrical conductivities are governed by their valence band, the width of which is determined by the distance and the staggering angle between two successive rings. These two essential parameters in ZnPcCl are similar to those of conductive compounds.[3] The good conductivity of ZnPcCl, despite an integral oxidation state, is obviously the consequence (i) of the very efficient overlap between Pc macrocycles (3.16 Å) associated in $(ZnPc)_2$ dimeric units and (ii) of the good mobility allowed by the small distance (3.38 Å) left between the aromatic regions of two adjacent units in the helical stacking. It is noticeable that this structure presents similarities to both types of stacked materials. At first sight the structure appears as an alternating stack of $Cl^-(ZnPc)_2^{2+}Cl^-$ units. But it could as well be interpreted as two segregated stacks, one stack consisting of a $(ZnPc)_2$ continuous helix with a mean distance between planes comparable to the Pc–Pc distance in $NiPcI_{1.0}$, the other stack being an helix

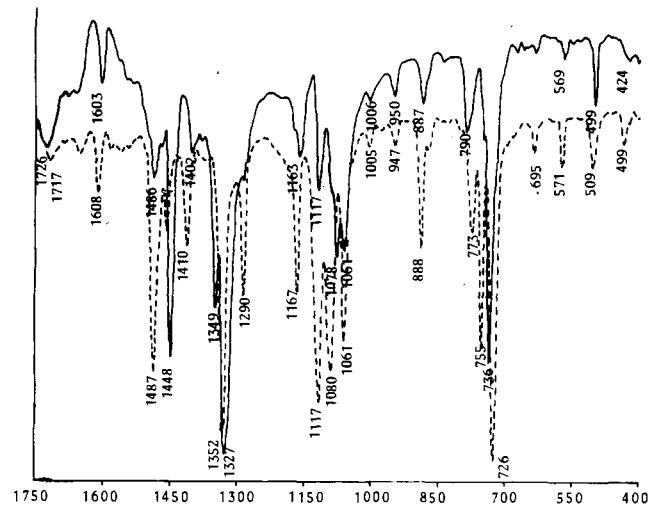


**Figure 5.** Infrared spectra of $ZnPc^+$ (—) and α-ZnPc (---).

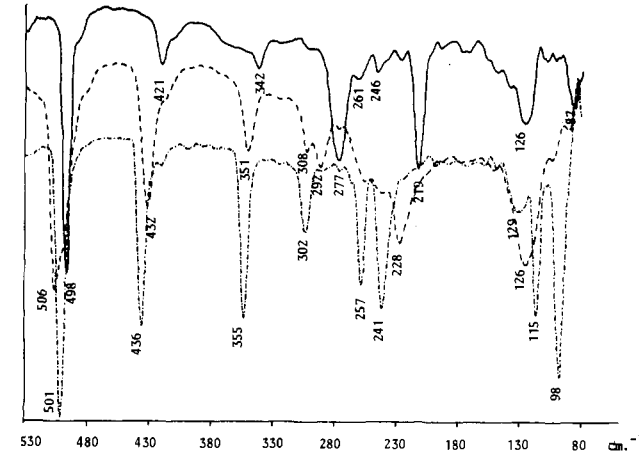


**Figure 6.** Infrared spectra of $ZnPc^+$ (—), α-ZnPc (---), and β-ZnPc (-·-·). α-ZnPc contains traces of β-ZnPc.

of Cl anions that are much less mobile than the $I_3^-$ groups in the $NiPcI_{1.0}$ channels.

**Infrared Spectra.** While reports on ZnPcCl are rather limited and unprecise,[20] both α and β modifications of ZnPc have been investigated in the 2000–200-cm$^{-1}$ range.[21] Kobayashi has reported on low-frequency vibrations of ZnPc.[22] Our samples gave FT-IR spectra identical with those published for α- and β-ZnPc; besides, our original data obtained by an improved technique cover the 500–80-cm$^{-1}$ range for α-ZnPc and for ZnPcCl.

Oxidation at the electrode induces important shifts in the spectra. These shifts can be observed in detail in Figures 5 and 6. Bands related mainly to C–C peripheral modes[21] remain almost unchanged (i.e. 1600, 1000, 947 and 500 cm$^{-1}$) and can be used as reference in the intensity comparisons. Metal-dependent absorptions undergo important alterations in size and/or position. This is obvious for ZnPc bands at 888, 1060, and 1285 cm$^{-1}$ as well as in the 1410–1486-cm$^{-1}$ cluster. Some other modes are given as stacking dependent[23] and are shifted in the $(ZnPc)_2Cl_2$ spectra, in the 1060–1160-cm$^{-1}$ region, at 753 and at 726 cm$^{-1}$ (CH out-of-plane bending[21]). Low-frequency vibrations are compared in Figure 6, the 500-cm$^{-1}$ band being used as reference. Variations between α and β modifications are minor and affect

(18) Ibers, J. A.; Pace, L. J.; Martinsen, J.; Hoffman, B. M. *Struct. Bonding (Berlin)* **1982**, *50*, 1.
(19) Whangbo, M. H.; Stewart, K. R. *Isr. J. Chem.* **1983**, *23* (1), 133.
(20) Meyers, J. F.; Rayner Ganham, G. W.; Lever, A. B. P. *Inorg. Chem.* **1975**, *14*, 461.
(21) Sidorov, A. N.; Kotlyar, I. P. *Opt. Spectrosc. (Engl. Transl.)* **1961**, *11*, 175.
(22) Kobayashi, T. *Spectrochim. Acta, Part A* **1970**, *26A*, 1313.
(23) Iwatsu, F.; Kobayashi, T.; Uyeda, N. *J. Phys. Chem.* **1980**, *84*, 3223.
(24) Nohr, R. S.; Kuznesof, P. M.; Wynne, K. J.; Konney, M. E.; Siebenman, P. G. *J. Am. Chem. Soc.* **1981**, *103*, 4371.
(25) Marks, T. J.; Schoch, K. F., Jr.; Kundalar, B. R. *Synth. Met.* **1979/80**, *1*, 337.

the bands at 292/302 (aza nitrogens?[22]) 228/257-241, and 126/98-115 $cm^{-1}$ (Zn-N(macrocycle)), the $\alpha$ and $\beta$ modifications frequencies being respectively before and behind the slash. As these two forms differ only by the relative position of Pc planes, vibrations in $\beta$-ZnPc could be given as more sensitive to axial N(aza)-Zn interactions between adjacent molecules in the herringbone stacking. The same group of bands is much more altered in ZnPcCl. Considerable broadening or loss of intensity as well as frequency shifts is evident at 421, 341, 126, and 88 $cm^{-1}$. Three bands at 302, 261, and 246 $cm^{-1}$ nearly vanish. Two rather important and well-defined bands at 277 and 213 $cm^{-1}$ are good candidates for Zn-Cl stretching modes.[20] This would be consistent with the weak axial bond on Zn, characterized in the lattice cell. Spectra of the similar compounds ZnPcX ($X \neq Cl$) are currently being studied in our group and will help assign the absorptions in the low-frequency region for the stacked compounds of this series.

## Conclusion

Our investigation answers diverse proposals on the structure of ZnPcCl.[20] We have prepared this compound by an original procedure, rarely applied to this class of molecules, for which partial oxidation through iodine insertion looks to be the general way of access to semiconductive or metallic molecular material. FT-IR results are consistent with X-ray analysis data.

ZnPcCl owes its electrical properties (i) to the integral oxidation number of the bimolecular entity $(ZnPc)_2$, (ii) to the very close association and favorable staggering angle of Pc rings, (iii) to the limited but effective interaction between the aromatic rings of the $(ZnPc)_2$ blocks in the helical stacking, and (iv) to the limited mobility of the counteranions. This first example of undoped Pc semiconductors displays a distinct structural feature: the metal atom lies at a distance of 0.59 Å from the ring center. For similar complexes, the metal atom displacement from the ring center is always much smaller.

The main character of higher conductivity and lower activation energy is being investigated on the same type of ZnPcX crystals, electrodeposited in the presence of $NR_4^+X^-$ electrolytes. Improvements of preparative conditions are expected to yield large enough single crystals to perform a full study of the anisotropy.

**Registry No.** ZnPcCl, 53466-59-4.

**Supplementary Material Available:** Listings of structure factor amplitudes, root-mean-square amplitudes of thermal vibration, general temperature factor expressions ($U$'s), and torsional angles (in degrees) (7 pages). Ordering information is given on any current masthead page.

---

Contribution from the Department of Chemistry, Purdue University, West Lafayette, Indiana 47907

# Ligand Structural Influences upon Electrochemical Reactivity: Organic Substituent Effects upon (Carboxylato)pentaamminecobalt(III) Reductions at Mercury and Gold Electrodes

TOMI T.-T. LI and MICHAEL J. WEAVER*

*Received October 12, 1984*

The electroreduction kinetics of 33 (carboxylato)pentaamminecobalt(III) complexes containing a variety of aliphatic, aromatic, and heterocyclic substituents have been examined at mercury- and gold-aqueous interfaces and compared with the corresponding homogeneous reduction rates with $Ru(NH_3)_6^{2+}$ in order to examine the relationships between the substituent structure and electrochemical reactivity. Complexes having acyclic aliphatic groups yielded "normal" outer-sphere reactivities on the basis of their similar relative rate constants at a given electrode potential in comparison with the corresponding homogeneous rate ratios. However, electrochemical reactivities that are enhanced by ca. $10-10^4$-fold on this basis were observed for complexes with ring-containing substituents. The extent of these rate enhancements depended on the ring structure, the smallest (ca. 10-30-fold) being seen with aliphatic ring substituents and the largest ($200-10^3$-fold) for thiophenes, with intermediate values for reactants having furan, pyridine, and benzene groups. Similar unimolecular rate constants were nonetheless observed for the electroreduction of several of these complexes when electrostatically adsorbed at chloride-coated silver. This indicates that the observed catalysis at mercury and gold surfaces arises from reactant adsorption, i.e., from increased precursor stability, presumably associated with "hydrophobic" or van der Waals ligand-surface interactions. "Normal" outer-sphere electroreduction pathways were observed, however, at mercury electrodes in several aprotic solvents, as deduced from the common correlation between the electrochemical reactivities and the inductive substituent parameter. A similar correlation is seen for the $Ru(NH_3)_6^{2+}$ reduction kinetics in aqueous solution.

## Introduction

We have recently been examining the kinetics of simple electrochemical reactions involving transition-metal systems, primarily Co(III)/Co(II), Cr(III)/Cr(II), and Ru(III)/Ru(II) couples at a variety of metal-solution interfaces.[1] One objective is to evaluate how the rates and mechanisms of heterogeneous electron-transfer reactions are influenced by the coordinated ligand structure, especially in relation to the detailed picture of reactant structural effects that has emerged for reactions between metal complexes in homogeneous solution.[2] Similarly to homogeneous processes, such electrochemical reactions commonly occur via inner-sphere mechanisms where a coordinated ligand is bound directly in the transition state for electron transfer.[2a] Not surprisingly, the kinetics of such inner-sphere reactions are often extremely sensitive to both the nature of the metal surface and to the bridging ligand.[1f-h,2c]

By analogy with homogeneous processes, outer-sphere electrochemical mechanisms are anticipated for reactants that lack a functional group capable of binding to the metal surface. Thus, electron transfer involving such species is expected to occur without the coordinated ligands penetrating the inner layer of solvent molecules adjacent to the electrode surface (the electrode's "coordination layer").[2a] One therefore might expect that the

(1) For example, see the following and references cited therein: (a) Barr, S. W.; Guyer, K. L.; Weaver, M. J. *J. Electroanal. Chem. Interfacial Electrochem.* **1980**, *111*, 41. (b) Weaver, M. J. *J. Phys. Chem.* **1980**, *84*, 568. (c) Weaver, M. J.; Tyma, P. D.; Nettles, S. M. *J. Electroanal. Chem. Interfacial Electrochem.* **1980**, *114*, 53. (d) Srinivasan, V.; Barr, S. W.; Weaver, M. J. *Inorg. Chem.* **1982**, *21*, 3154. (e) Hupp, J. T.; Weaver, M. J. *Inorg. Chem.* **1983**, *22*, 2557. (f) Barr, S. W.; Weaver, M. J. *Inorg. Chem.* **1984**, *23*, 1657. (g) Guyer, K. L.; Weaver, M. J. *Inorg. Chem.* **1984**, *23*, 1657. (h) Li, T. T.-T.; Liu, H. Y.; Weaver, M. J. *J. Am. Chem. Soc.* **1984**, *106*, 1233.

(2) (a) Weaver, M. J. *Isr. J. Chem.* **1979**, *18*, 35. (b) Weaver, M. J.; Hupp, J. T. *ACS Symp. Ser.* **1982**, *No. 198*. 181. (c) Barr, S. W.; Guyer, K. L.; Li, T. T.-T.; Liu, H. Y.; Weaver, M. J. *J. Electrochem. Soc.* **1984**, *131*, 1626. (d) Hupp, J. T.; Liu, H. Y.; Farmer, J. K.; Gennett, T.; Weaver, M. J. *J. Electroanal. Chem. Interfacial Electrochem.* **1984**, *168*, 313. (e) Hupp, J. T.; Weaver, M. J. *J. Phys. Chem.*, in press.

0020-1669/85/1324-1882$01.50/0 